

## 1

## On the Track of Reaction Mechanisms: Characterization and Reactivity of Metal Atom Dimers

Hans-Jörg Himmel

## 1.1

### Introduction

The matrix-isolation technique is now well established as a valuable method to retain and characterize reaction intermediates [1]. In this chapter, it will be shown how this method can be used to characterize metal atom dimers and to shed light on their special reactivity. An understanding of the bond properties and reactivities of these metal atom dimers is a first step toward an understanding of the physical and chemical properties of metal atom clusters. Because of their high reactivity, metal atom clusters are widely used for catalytic processes. In addition, larger clusters with a diameter in the nm range (ideally 1–2 nm) exhibit quantum-size effects, which make their use in single-electron devices attractive. In spite of these wide-ranging applications, detailed information about the structures and electronic properties of metal atom clusters is sparse. There are not only experimental difficulties. Quantum chemical calculations become extremely difficult and expensive, even in the case of the metal atom dimers. Multi-reference methods have to be applied and inner-core correlation has to be taken into account. Often DFT methods fail or are not really reliable.

Although clusters are generally more reactive than metal atoms or ideal defect-free surfaces, first results show that there are large differences between clusters that consist of different numbers of atoms. In some cases, the maximum reactivity of an  $M_n$  particle (where  $M$  denotes a metal atom and  $n \geq 1$ ) seems to be reached at the stage of the metal atom dimer. Thus, gas-phase studies revealed that  $Rh_2^+$  brings about a spontaneous dehydrogenation reaction with  $CH_4$ , while  $Rh^+$  ions and  $Rh_n^+$  clusters ( $n \geq 3$ ) do not induce spontaneous reaction [2]. In the same vein,  $Pt_2^+$ , but not  $Pt^+$  ions or  $Pt_n^+$  clusters, were found to react with  $NH_3$  to give the dehydrogenation product  $[Pt_2NH]^+$  [3].

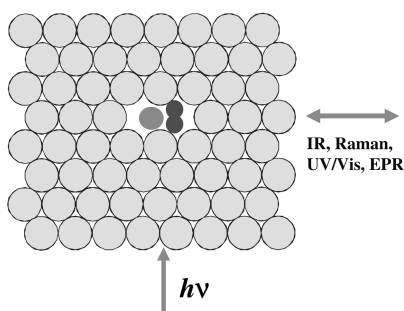
After a brief description of the matrix-isolation technique, the results which have led to a detailed characterization of  $Ga_2$  and  $Ti_2$  will be reported. Thereafter, the reactions between  $Ga_2$  and  $H_2$  and between  $Ti_2$  and  $N_2$  are discussed. These two model reactions underline impressively the high reactivity of metal atom dimers.

## 1.2

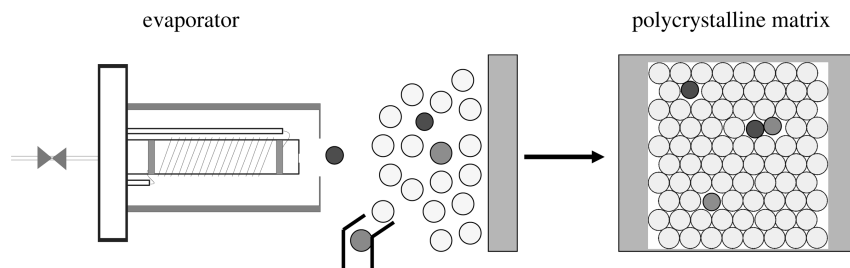
**Principle and Realization of the Matrix-Isolation Experiment**

In the matrix-isolation experiment, the two reactants are isolated in a host material, which generally consists of a frozen inert gas (e.g. argon) to minimize chemical interactions between the host and the isolated reactants (Fig. 1.1). The temperature is kept very low (at a few Kelvin). At these temperatures, even small reaction barriers (of a few  $\text{kJ mol}^{-1}$ ) cannot easily be surmounted ( $kT=0.08 \text{ kJ mol}^{-1}$  at 10 K), if tunnelling processes can be neglected. Therefore, reaction intermediates that cannot survive under other conditions can be generated, trapped, and observed. Indeed, one of the great advantages of the matrix-isolation method is that the reaction intermediates can be retained for several hours or even days and therefore can be identified and characterized at leisure by applying standard laboratory techniques.

The identification and characterization of possible intermediates and reaction products usually relies on spectroscopic methods. Vibrational spectroscopy is certainly the most widely applied method, combining as it does the advantages of high sensitivity and the provision of information that can not only be used to identify the species, but also to determine some important properties such as symmetry and more detailed structural information, force constants, and, in some cases, dissociation energies (see below). To allow for a better analysis of the data, the experiments have to be repeated with as many isotopomers as possible. These isotopomers usually have to be synthesized especially for this purpose. The experimental results are often accompanied by quantum chemical calculations, which allow for a further characterization. Absorption spectroscopy with radiation energy sufficiently high to excite electrons within the species isolated in the matrix provides valuable information about possible photochemistry and may be used to analyze the properties of excited states. Thus, if the spectra are vibrationally resolved, the frequency and important structural information can be obtained for some excited states of the species under investigation. Fluorescence spectroscopy can also be extremely informative, although this technique can only be applied in certain cases. Finally, radicals might be studied by means of EPR spectroscopy (see ref. [1] for more information on possible methods of interrogation).



**Fig. 1.1** Two reactants are isolated in a defect of the polycrystalline matrix host material. The spontaneous and photolytically induced reactions can be followed by means of spectroscopic methods, such as absorption (vibrational or electronic excitations), emission, or EPR spectroscopy.



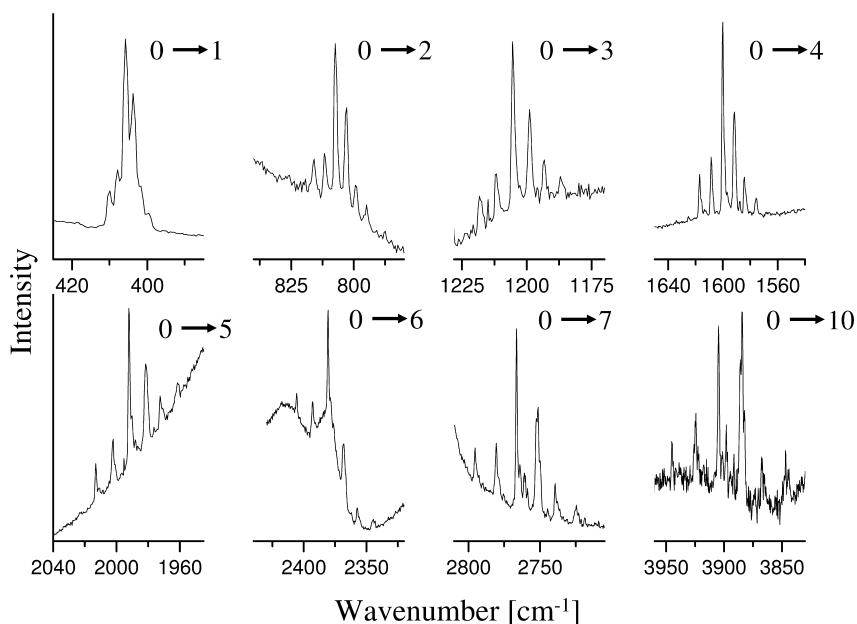
**Fig. 1.2** Preparation of a matrix which contains two reactants. One of them is produced in an evaporator, the second is admixed to the matrix gas. The result is a statistical distribution of the two reactants in defect sites of the matrix host.

Fig. 1.2 illustrates the preparation of a matrix in a typical matrix experiment. In the studies discussed herein, one of the reactants is emitted from a metal evaporator. For example, gallium vapor can be generated by resistively heating the metal in a BN cell, or an alumina tube containing a carbon cell, to a temperature of 900–1000 °C. An element like titanium, for which higher temperatures are necessary, may be evaporated by directly heating a pure metal wire (to 1600–1700 °C in the case of titanium). The amount of deposited metal can be monitored with the aid of a microbalance. The other reactant is admixed to the matrix gas. The matrix is deposited onto a metal block (e.g., Cu or Rh-plated Cu) kept at a low temperature (10 K in general), generally by means of a closed-cycle refrigerator. UV/Vis spectra give useful information about the metal atom to metal atom dimer ratio in the matrix.

### 1.3 Characterization of Metal Atom Dimers

Metal atom dimers in a matrix can be characterized by means of absorption (e.g. UV/Vis), resonance-Raman, and/or fluorescence spectroscopy. In some cases, the resonance-Raman spectra reveal not only the  $\nu(\text{M-M})$  stretching fundamental, but also several overtones. These overtones can be used to estimate the dissociation energy, which is an important parameter in describing the metal–metal bond. It is also of importance for the understanding of reaction mechanisms, since the metal–metal bond is often ruptured in the course of the reaction. Thus, the energy required for the rupture of the metal–metal bond has to be compensated by the formation of other bonds if the reaction is to proceed spontaneously. In the following, the results obtained for  $\text{Ti}_2$  and  $\text{Ga}_2$  from matrix-isolation experiments and quantum chemical calculations are discussed. These two metal atom dimers were chosen exemplarily because, as detailed below, they show remarkably high reactivities.

**Ti<sub>2</sub>** Fig. 1.3 shows the resonance-Raman spectra obtained for  $\text{Ti}_2$  measured with the  $\lambda = 514.532$  nm line of an  $\text{Ar}^+$  ion laser [4]. Some regions of the spectrum are



**Fig. 1.3** Resonance Raman spectra of  $\text{Ti}_2$  isolated in an Ar matrix (measured with the 514.532 nm line of an  $\text{Ar}^+$  ion laser).

covered by fluorescence signals, which for the most part belong to Ti atoms. Nevertheless, in the regions free from fluorescence signals, a series of overtones can be measured, which exhibit an isotopic splitting. The results can be used to estimate the dissociation energy on the basis of a LeRoy–Bernstein–Lam analysis [5]. In this analysis, the potential near the dissociation limit is assumed to be a quadrupole–quadrupole-type interaction between two Ti atoms in their  $^3F$  electronic ground state. One then interpolates between the formulas derived for the vibrational level energies near the dissociation limit (resulting from a WKB treatment) and those that are closer to the bottom of the potential-energy curve. The analysis yields a dissociation energy ( $D_e$  value) of  $113.9 \text{ kJ mol}^{-1}$  [4].

Additional valuable information is provided by absorption measurements. Fig. 1.4 shows the absorption spectrum of  $\text{Ti}_2$  in the region between  $4000$  and  $6500 \text{ cm}^{-1}$  [6]. Two series of bands are visible, which can be assigned to excitations into different vibrational levels of the  $1^3\Pi_u$  and the  $1^3\Phi_u$  states. The relative intensities of the bands in each series can be used to estimate the difference  $\Delta r_e$  in the bond distances between the excited state and the ground state on the basis of a Franck–Condon analysis. To this end, Morse-type functions were assumed for each state. The analysis resulted in  $\Delta r_e$  values of  $9 \text{ pm}$  for the  $1^3\Pi_u \leftarrow ^3\Delta_g$  and of  $10 \text{ pm}$  for the  $1^3\Phi_u \leftarrow ^3\Delta_g$  transition. Thus, the Ti–Ti bond length is found to increase in both electronically excited states relative to the ground state.

Experimental information was also obtained for the next higher  $2^3\Pi_u$  and  $2^3\Phi_u$  states. In these states, the Ti–Ti bond is even longer. Tab. 1.1 includes  $\Delta r_e$ ,

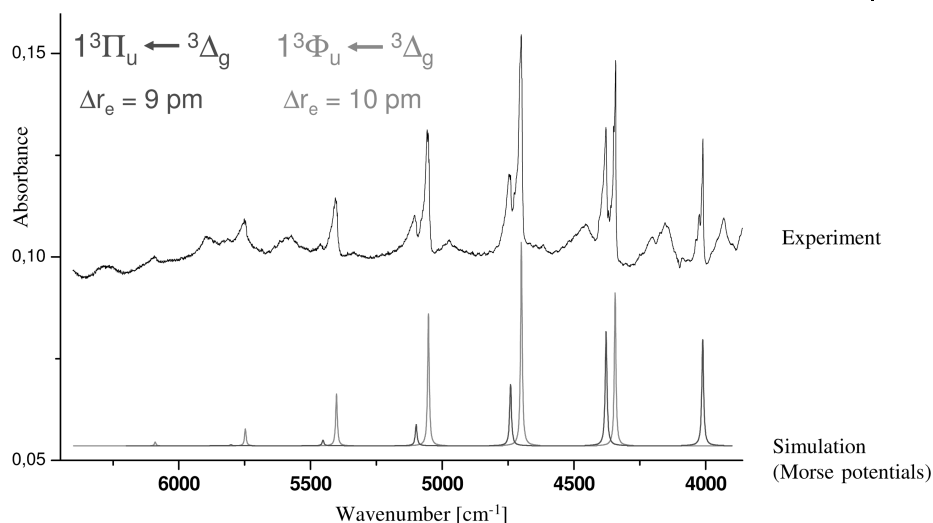


Fig. 1.4 Absorption spectrum of  $\text{Ti}_2$  in the region between 4000 and 6500  $\text{cm}^{-1}$ . The bands are due to two vibrationally resolved electronic excitations.

Tab. 1.1 Comparison between the experimentally determined and calculated [MRCI (ANO 76432)] relative bond distances  $\Delta r_e$  (in pm), the harmonically corrected frequencies, and the excitation energies  $T_e$  (in  $\text{kJ mol}^{-1}$ )

Electronic state	$\Delta r_e$		$\omega_e$		$T_e$	
	exp.	calcd.	exp.	calcd.	exp.	calcd.
${}^3\Delta_g$	0	0	407.0	369	0	0
$1\ {}^3\Pi_u$	$9 \pm 2$	11.3	371.5	330	48.2	40.5
$1\ {}^3\Phi_u$	$10 \pm 2$	12.2	359.5	317	52.1	42.5
$2\ {}^3\Pi_u$	$13 \pm 2$	17.4	282.0	259	83.9	71.4
$2\ {}^3\Phi_u$	$13 \pm 4$	17.0	288.2	268	99.4	91.7

the harmonic frequencies  $\omega_e$ , and the excitation energies  $T_e$  for all states for which detailed experimental information is available. Tab. 1.1 also compares the experimentally derived values with those predicted by high-level quantum chemical calculations (MRCI method).

**Ga<sub>2</sub>** Again, resonance-Raman spectroscopy proves to be extremely useful to obtain information about the ground state of the dimer. The resonance-Raman spectrum of  $\text{Ga}_2$  is displayed in Fig. 1.5 [7]. The  $\nu(\text{Ga-Ga})$  stretching fundamental occurs at 176.5  $\text{cm}^{-1}$ . Three additional signals in the spectrum can be assigned to the first, second and third overtones. The signals show an isotopic

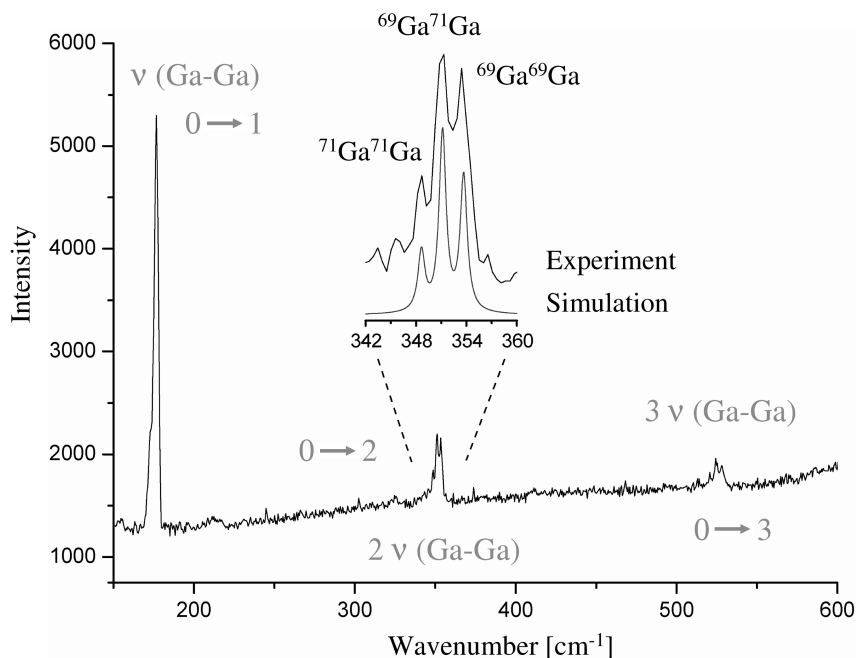


**Fig. 1.5** Resonance Raman spectrum of  $\text{Ga}_2$ , obtained with the 514.532 nm line of an  $\text{Ar}^+$  ion laser.

**Tab. 1.2** Calculated dimensions (in pm), harmonic vibrational frequencies (in  $\text{cm}^{-1}$ ), and relative energies (in  $\text{kJ mol}^{-1}$ ) of  $\text{Ga}_2$  in various electronic states

$\text{Ga}_2$		CASSCF/SVP	MP2/TZVPP	Exp.
$^3\Pi_u$	$d(\text{Ga-Ga})$	276.3	271.4	
	$\omega(\text{Ga-Ga})$	161	178	175
$^3\Sigma_g^-$	$\Delta E$	7.1	7.8	
	$d(\text{Ga-Ga})$	251.0	247.1	
$^1\Sigma_g^+$	$\omega(\text{Ga-Ga})$	204	222	
	$\Delta E$	19.0	41.5	
	$d(\text{Ga-Ga})$	309.3	300.3	
$^1\Pi_u$	$\omega(\text{Ga-Ga})$	121	146	
	$\Delta E$	46.3		
	$d(\text{Ga-Ga})$	278.1		
$^1\Delta_g$	$\omega(\text{Ga-Ga})$	154		
	$\Delta E$	56.4		
	$d(\text{Ga-Ga})$	258.7		
	$\omega(\text{Ga-Ga})$	170		

splitting that is in pleasing agreement with the pattern expected for  $\text{Ga}_2$  (see inset in Fig. 1.5) in its three isotopic forms  $^{69}\text{Ga}^{69}\text{Ga}$ ,  $^{69}\text{Ga}^{71}\text{Ga}$ , and  $^{71}\text{Ga}^{71}\text{Ga}$ . The dissociation energy of  $\text{Ga}_2$  can be estimated to be ca.  $130 \text{ kJ mol}^{-1}$ .

Unfortunately, it has hitherto not been possible to obtain detailed information about excited states of  $\text{Ga}_2$  with energies close to the ground state. Calculations indicate that a  $^3\Sigma_g^-$  state has an energy which is only ca.  $7 \text{ kJ mol}^{-1}$  higher than that of the  $^3\Pi_u$  ground state. Several singlet states are also predicted to be close by in energy (see Tab. 1.2) [10]. It will be shown below that these excited states play a significant role in relation to the reactivity of  $\text{Ga}_2$ .

## 1.4

### Reactivity of Metal Atom Dimers and Comparison with the Reactivity of Single Metal Atoms

In the following, two examples are discussed which should underline the strikingly high reactivity of metal atom dimers, namely the reaction of  $\text{Ga}_2$  with  $\text{H}_2$  and the reaction of  $\text{Ti}_2$  with  $\text{N}_2$ . Both reactions proceed spontaneously with the metal atom dimers in their ground electronic states.

#### 1.4.1

##### The Reaction Between $\text{Ga}_2$ and $\text{H}_2$

Ga atoms in their electronic ground state ( $^2\text{P}$ ) do not react with dihydrogen. A reaction can only be brought about by photoactivation of the Ga atoms ( $^2\text{S} \leftarrow ^2\text{P}$  excitation), thereby leading to the bent radical  $\text{GaH}_2$  [8, 9]. This result is at first glance surprising, since transition metal atoms are known to react spontaneously with  $\text{H}_2$  only after one of the d electrons has been excited into an empty p orbital. On this basis, it has been argued that the attractive interaction between the half-filled p orbital and the  $\sigma^*$  orbitals at the dihydrogen initiates the reaction. A correlation diagram shows, however, that the ground state of the  $\text{Ga}\cdots\text{H}_2$  system (with a large separation between Ga and  $\text{H}_2$ ) correlates with an excited state of the product  $\text{GaH}_2$ . Therefore, the thermal reaction is subject to a massive reconfiguration barrier [10]. In fact, a radical mechanism is favored, which leads first to GaH and H atoms, and these combine in the second step to give the  $\text{GaH}_2$  radical. Thus, although the overall reaction is slightly endothermic (by  $16 \text{ kJ mol}^{-1}$  according to MP2/TZVPP), [10] photolysis is needed for the reaction to take place.

For the reaction between  $\text{Ga}_2$  and  $\text{H}_2$ , one might also assume at first glance a significant barrier, since the reaction is formally spin-forbidden ( $\text{Ga}_2$  exhibits a triplet ground electronic state and  $\text{Ga}_2\text{H}_2$  a singlet one). However, spin-orbit coupling is significant and provides a means by which the system can change its multiplicity from triplet to singlet. The experiments show that  $\text{Ga}_2$  reacts spontaneously with  $\text{H}_2$  to give the cyclic,  $D_{2h}$  symmetric  $\text{Ga}(\mu\text{-H})_2\text{Ga}$  molecule (see Fig. 1.6) [10]. Calculations indicate that the reaction proceeds via excited states of  $\text{Ga}_2$ . Thus, in the early stage of the approach between the two reactants, the  $^3\Pi_u$  and  $^3\Sigma_g^-$  type states

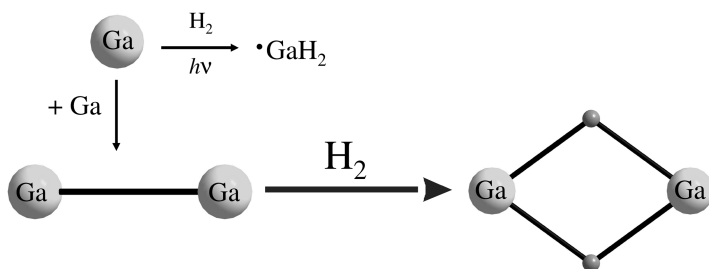


**Fig. 1.6** Ga<sub>2</sub> reacts spontaneously with H<sub>2</sub> to give the cyclic, D<sub>2h</sub> symmetric Ga(μ-H)<sub>2</sub>Ga ring. Ga atoms react with H<sub>2</sub> only upon photoactivation, the product being the bent radical GaH<sub>2</sub>.

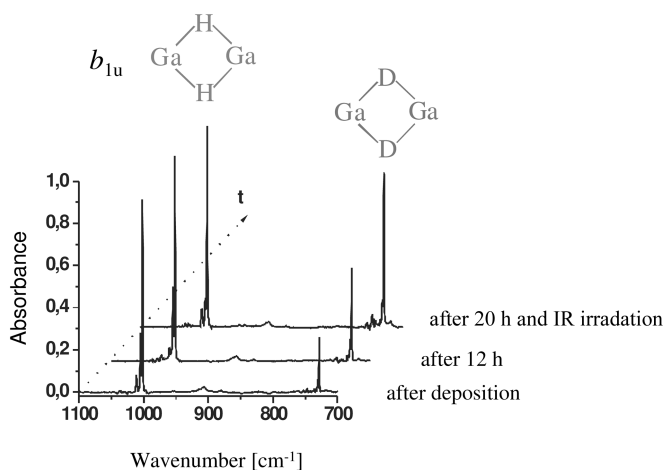


**Fig. 1.7** IR spectra taken for an Ar matrix containing Ga<sub>2</sub> and a 1:1 mixture of H<sub>2</sub>/D<sub>2</sub>.

of Ga<sub>2</sub> mix. At the point of intersystem crossing from triplet to singlet state, a <sup>1</sup>Δ<sub>g</sub> type state is adopted. As a consequence, the Ga–Ga distance first shortens from 276 to 255 pm. The relevant excited states have energies which are relatively close to that of the ground state. Therefore, the barrier to reaction is relatively low. The experiments give additional information about the reaction mechanism. Thus, the reaction proceeds spontaneously with H<sub>2</sub>, but not with D<sub>2</sub>. In the case of D<sub>2</sub>, the matrix has to be kept for several hours in the dark or irradiated with IR light to complete the reaction (see Fig. 1.7). This isotopic effect indicates that the barrier to reaction is of the order of the zero-point energy difference between H<sub>2</sub> and D<sub>2</sub>, viz. ca. 30 kJ mol<sup>-1</sup>. This value is slightly lower than the calculated estimate (ca. 50 kJ mol<sup>-1</sup>). Nevertheless, both experiment and theory agree in that Ga<sub>2</sub> is much more reactive toward H<sub>2</sub> than a single Ga atom.

It is worth mentioning that Ga(μ-H)<sub>2</sub>Ga can be converted into two other isomeric forms when the molecule is selectively photolyzed (see Fig. 1.8). In both

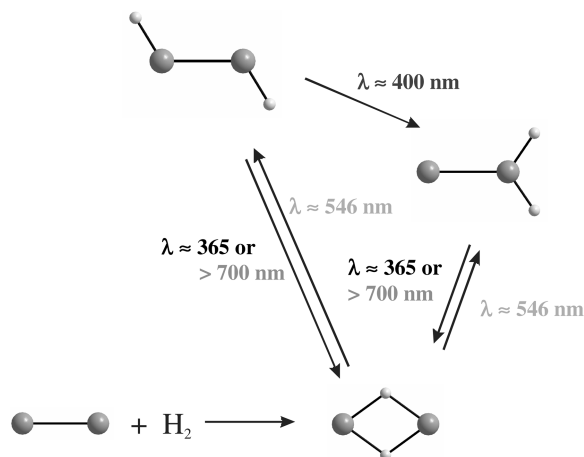
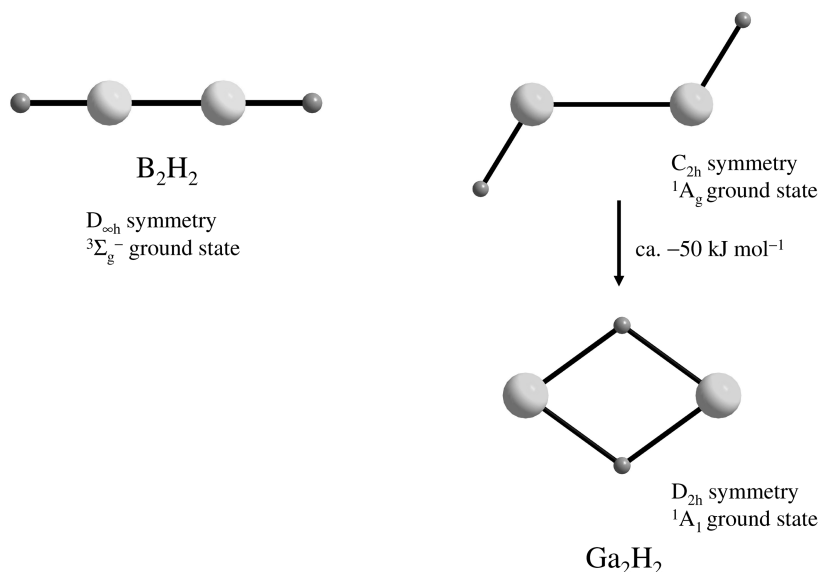


Fig. 1.8 Photoconversion of Ga(μ-H)<sub>2</sub>Ga into the two isomers HGaGaH and GaGaH<sub>2</sub>.

of these isomers, direct Ga–Ga bonds exist. One of the isomers is the *trans*-bent species HGa–GaH. Analysis of the spectra obtained for this molecule in combination with quantum chemical calculations clearly shows that the Ga–Ga bond is most adequately described as a relatively weak donor–acceptor interaction between two GaH diatomics. According to quantum chemical calculations, the energy for fragmentation of HGa–GaH into two non-relaxed GaH units with singlet electronic state amounts to no more than 57 kJ mol<sup>-1</sup> [11]. This again shows that the Ga–Ga bond is weak. At 262.0 pm, the calculated Ga–Ga bond distance is relatively long. Meanwhile, there are structural data (from X-ray diffraction analyses) available for some derivatives Ar'GaGaAr' (e.g., with Ar' being 2,6-Dipp<sub>2</sub>C<sub>6</sub>H<sub>3</sub>, Dipp = 2,6-*i*Pr<sub>2</sub>C<sub>6</sub>H<sub>3</sub>) [12, 13]. These data confirm the analysis made for HGaGaH. Like HGaGaH, the derivatives exhibit a *trans*-bent structure. The Ga–Ga bond distance in Ar'GaGaAr' amounts to 262.68(7) pm. The results also indicate that the Ga–Ga bond in the dianion [HGaGaH]<sup>2-</sup> cannot be adequately described as a triple bond and thus the properties differ to a large extent from those found for HCCH. This is also reflected in the different structures (*trans*-bent in the case of [HGaGaH]<sup>2-</sup> vs. linear for HCCH). The crystal structures of derivatives [RGaGaR]<sup>2-</sup> [e.g., R being 2,6-(2,6-*i*Pr<sub>2</sub>C<sub>6</sub>H<sub>3</sub>)<sub>2</sub>C<sub>6</sub>H<sub>3</sub>] [14] were determined and the Ga–Ga distance was found to be short (231.9 pm). However, this short distance does not necessarily imply the presence of a triple bond. An analysis indicates that the Na<sup>+</sup> cations are engaged in the bonding [15, 16]. At the same time, the Na<sup>+</sup> ion interacts with the aromatic rings on the ligands. That the Ga–Ga bond length has to be taken with caution as a criterion for the bond order also becomes evident if the values determined for typical Ga–Ga single bonds are compared. Thus, in Ga<sub>2</sub>[Ga<sub>2</sub>I<sub>6</sub>], the Ga–Ga bond length is 238.7(5) pm [17]. At the other extreme, a value of 254.1(1) pm was determined in the case of Ga<sub>2</sub>(Trip)<sub>4</sub> (Trip = 2,4,6-*i*Pr<sub>3</sub>C<sub>6</sub>H<sub>2</sub>) [18] and also for Ga<sub>2</sub>[CH(SiMe<sub>3</sub>)<sub>2</sub>]<sub>4</sub> [19].



**Fig. 1.9** Comparison between the structures of  $B_2H_2$  and its homologue  $Ga_2H_2$ .

In contrast to  $HGaGaH$ , the lighter homologue  $HBBH$  is a linear molecule with a triplet electronic ground state (see Fig. 1.9). The molecule has been characterized in matrix by IR [20] and EPR [21] spectroscopies, and has also been the subject of theoretical work [22]. The results show that, as anticipated, the triplet state arises from the presence of two degenerate  $\pi$ -orbitals, which are each occupied by one electron. The B–B bond is strong (in line with a formal bond order of 2) and the calculated B–B distance amounts to 150.7 pm. Fragmentation of  $HBBH$  into two geometrically non-relaxed HB units with singlet electronic states requires ca.  $450 \text{ kJ mol}^{-1}$  [CCSD(T) estimate] [11]. Nevertheless, the dimerization of the molecule to give  $B_4H_4$  in its tetrahedral global energy minimum structure is predicted to be highly exothermic [ca.  $-482 \text{ kJ mol}^{-1}$  according to CCSD(T) calculations] [23].

Recently, it has been shown that  $Ga_2$  reacts spontaneously not only with  $H_2$ , but also with  $SiH_4$  [24]. Interestingly, the product formed in this reaction is  $HGa(\mu\text{-}SiH_3)Ga$ , featuring a terminal Ga–H bond and the  $SiH_3$  group in a bridging position.

#### 1.4.2

#### The Reaction Between $Ti_2$ and $N_2$

According to matrix experiments, Ti atoms in their electronic ground state do not engage in a complex with dinitrogen.  $Ti_2$  dimers, however, undergo spontaneous reaction with  $N_2$ . In the course of this reaction, which proceeds without

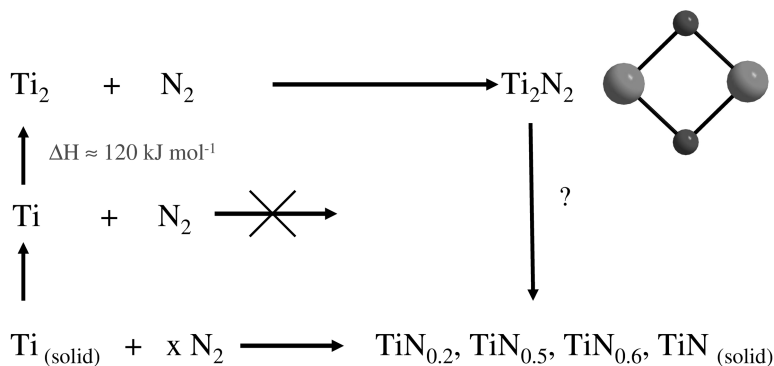


**Fig. 1.10** The reaction between  $\text{Ti}_2$  and  $\text{N}_2$  leads to the cyclic  $\text{Ti}(\mu\text{-N})_2\text{Ti}$  molecule, which might be an intermediate on the way to solid nitrides of titanium.

a significant barrier, four Ti–N bonds are formed at the expense of the strong NN triple bond, leading to a cyclic  $\text{Ti}(\mu\text{-N})_2\text{Ti}$  molecule (see Fig. 1.10) [25]. The spectra indicate that the product features no direct N–N interaction. The ground state of  $\text{Ti}(\mu\text{-N})_2\text{Ti}$  is a singlet state, but a triplet state is of very similar energy. It was possible to detect some vibrationally resolved excitations around  $9000 \text{ cm}^{-1}$  attributable to this species [25]. This reaction is especially interesting since solid Ti has been shown to react at higher temperatures with molecular nitrogen to first give compounds which contain N atoms dissolved in solid titanium ( $\text{TiN}_{0.20}$  intercalation compound), with the h.c.p. structure of  $\alpha$ -Ti. Finally, with increasing concentration of nitrogen and at ca.  $900^\circ\text{C}$ , a defect NaCl structure is adopted. Thus, in the course of this reaction, the NN bond of dinitrogen has to be ruptured.  $\text{Ti}_2\text{N}_2$  might be a possible intermediate on the way to these solid phases. A goal of future studies should be the estimation of the reaction enthalpy of  $\text{Ti}_2\text{N}_2$  formation. This value could then be used to calculate the enthalpy difference between  $\text{Ti}_2\text{N}_2$  and solid titanium nitride. Solid titanium nitride coatings are of interest as protection layers and as semiconductors.

The isodesmic reaction  $2 \text{TiCl}_4 + \text{Si}_2\text{N}_2 \rightarrow 2 \text{SiCl}_4 + \text{Ti}_2\text{N}_2$  can be used to estimate the standard enthalpy of formation for  $\text{Ti}_2\text{N}_2$ . This reaction was calculated to be exothermic by  $-194 \text{ kJ mol}^{-1}$ . First, the enthalpy of formation for  $\text{Si}_2\text{N}_2$  has to be estimated. The enthalpy for the reaction  $2\text{Si}(\text{g}) + \text{N}_2(\text{g}) \rightarrow \text{Si}_2\text{N}_2(\text{g})$  was calculated to be ca.  $-650 \text{ kJ mol}^{-1}$  [26]. With values of  $+450 \text{ kJ mol}^{-1}$  for the standard enthalpy of formation for  $\text{Si}(\text{g})$  [27], the standard enthalpy of formation of  $\text{Si}_2\text{N}_2$  amounts to ca.  $+250 \text{ kJ mol}^{-1}$ . With this value, the standard enthalpy of formation of  $\text{Ti}_2\text{N}_2(\text{g})$  can be estimated to be of the order of  $-49 \text{ kJ mol}^{-1}$  (with values of  $-763.2$  and  $-662.8 \text{ kJ mol}^{-1}$  for the standard enthalpies of formation of  $\text{TiCl}_4$  and  $\text{SiCl}_4$ , respectively [27]). Considering a value of  $945.4 \text{ kJ mol}^{-1}$  for the standard enthalpy of formation of two single N atoms, this value demonstrates the high affinity of titanium for nitrogen.

It also implies that the reaction between  $\text{Ti}_2(\text{g})$  (for which the enthalpy of formation is ca.  $+827 \text{ kJ mol}^{-1}$ ) and  $\text{N}_2$  has to be highly exothermic (standard reaction enthalpy ca.  $-876 \text{ kJ mol}^{-1}$ ). The enthalpy of formation of solid  $\text{TiN}$  was determined to be  $-337.7 \text{ kJ mol}^{-1}$ . Thus, the enthalpy for the reaction  $2 \text{ Ti}(\text{s}) + \text{N}_2 \rightarrow 2 \text{ TiN}(\text{s})$  amounts to  $-675.4 \text{ kJ mol}^{-1}$ . This value is smaller than the  $-876 \text{ kJ mol}^{-1}$  estimated for the enthalpy of formation of  $\text{Ti}_2\text{N}_2(\text{g})$  from  $\text{Ti}_2(\text{g})$  and  $\text{N}_2$ . These considerations do not prove, but support the view that the barrier for the formation of solid  $\text{TiN}$  from solid  $\text{Ti}$  and  $\text{N}_2$  is caused by the thermal energy required to form “ $\text{Ti}_2$ ” or other small clusters from solid  $\text{Ti}$ . According to these calculations,  $\text{Ti}_2\text{N}_2$  could very well be an intermediate on the way to solid titanium nitride.

## 1.5

### Concluding Remarks

The examples discussed herein demonstrate impressively how reactive metal atom dimers are. Electronically excited states with energies close to the ground state are often responsible for these high reactivities (as shown explicitly for the reaction between  $\text{Ga}_2$  and  $\text{H}_2$ ) [10]. Therefore, an understanding of the reaction mechanisms requires knowledge of the properties of the ground state and the excited states of these species. A detailed characterization can only be achieved through a combination of experimental and quantum chemical results. However, calculations are extremely difficult and multi-reference methods have to be applied. Inner-core correlation effects have to be rigorously included. As regards experiments, absorption and Raman spectroscopies have been shown to provide useful information on the matrix-isolated species.

The aims of future studies include the characterization of metal atom trimers and other small clusters and the analysis of their reactivity. The clusters can be generated by diffusion of metal atoms or dimers into the matrix upon annealing. Many new fascinating results are expected to emerge from these studies. They might prove to be valuable for possible applications in materials science and catalytic processes.

### References

- 1 See, for example: H.-J. HIMMEL, A. J. DOWNS, T. M. GREENE, *Chem. Rev.* **2002**, *102*, 4191.
- 2 ALBERT, C. BERG, M. BEYER, U. ACHATZ, S. JOOS, G. NIEDNER-SCHATTEBURG, V. E. BONDYBEY, *Chem. Phys. Lett.* **1997**, *268*, 235.
- 3 K. KOSZINOWSKI, D. SCHRÖDER, H. SCHWARZ, *J. Phys. Chem. A* **2003**, *107*, 4999.
- 4 H.-J. HIMMEL, A. BIHLMEIER, *Chem. Eur. J.* **2004**, *10*, 627.
- 5 See, for example: R. J. LE ROY, W.-H. LAM, *Chem. Phys. Lett.* **1980**, *71*, 544.

- 6 O. HÜBNER, H.-J. HIMMEL, W. KLOPPER, L. MANCERON, *J. Chem. Phys.*, **2004**, *121*, 7195.
- 7 H.-J. HIMMEL, B. GAERTNER, *Chem. Eur. J.* **2004**, *10*, 5936. See also a previous report: F. W. FROBEN, W. SCHULZE, U. KLOSS, *Chem. Phys. Lett.* **1983**, *99*, 500.
- 8 P. PULLUMBI, C. MIJOULE, L. MANCERON, Y. BOUTEILLER, *Chem. Phys.* **1994**, *185*, 13.
- 9 L. B. KNIGHT, JR., J. J. BANISAUKAS III, R. BABB, E. R. DAVIDSON, *J. Chem. Phys.* **1996**, *105*, 6607.
- 10 a) A. KÖHN, H.-J. HIMMEL, B. GAERTNER, *Chem. Eur. J.* **2003**, *9*, 3909. b) H.-J. HIMMEL, L. MANCERON, A. J. DOWNS, P. PULLUMBI, *Angew. Chem.* **2002**, *111*, 829; *Angew. Chem. Int. Ed.* **2002**, *41*, 796. c) H.-J. HIMMEL, C. MANCERON, A. J. DOWNS, P. PULLUMBI, *J. Am. Chem. Soc.* **2002**, *124*, 4448.
- 11 H.-J. HIMMEL, H. SCHNÖCKEL, *Chem. Eur. J.* **2003**, *9*, 748.
- 12 N. J. HARDMAN, R. J. WRIGHT, A. D. PHILLIPS, P. P. POWER, *Angew. Chem.* **2002**, *114*, 2966.
- 13 N. J. HARDMAN, R. J. WRIGHT, A. D. PHILLIPS, P. P. POWER, *J. Am. Chem. Soc.* **2003**, *125*, 2667.
- 14 J. SU, X. W. LI, R. C. CRITTENDON, G. H. ROBINSON, *J. Am. Chem. Soc.* **1997**, *119*, 5471.
- 15 N. TAKAGI, M. W. SCHMIDT, S. NAGASE, *Organometallics* **2001**, *20*, 1646.
- 16 H.-J. HIMMEL, H. SCHNÖCKEL, *Chem. Eur. J.* **2002**, *8*, 2397.
- 17 (a) J. C. BEAMISH, M. WILKINSON, I. J. WORRALL, *Inorg. Chem.* **1978**, *17*, 2026. (b) G. GERLACH, W. HÖNLE, A. SIMON, *Z. Anorg. Allg. Chem.* **1982**, *486*, 7.
- 18 X. HE, R. A. BARTLETT, M. M. OLMSTEAD, K. RUHLANDT-SENGE, R. W. STURGEON, P. P. POWER, *Angew. Chem.* **1993**, *105*, 761.
- 19 W. UHL, M. LAYH, T. HILDENBRAND, *J. Organomet. Chem.* **1989**, *364*, 289.
- 20 T. J. TAGUE, JR., L. ANDREWS, *J. Am. Chem. Soc.* **1994**, *116*, 4970.
- 21 L. B. KNIGHT, JR., K. KERR, P. K. MILLER, C. A. ARRINGTON, *J. Phys. Chem.* **1995**, *99*, 16842.
- 22 See, for example: (a) J. D. WATTS, R. J. BARTLETT, *J. Am. Chem. Soc.* **1995**, *117*, 825. (b) P. R. SCHREINER, H. F. SCHAEFER III, P. V. R. SCHLEYER, *J. Chem. Phys.* **1994**, *101*, 7625.
- 23 H.-J. HIMMEL, *Eur. J. Inorg. Chem.* **2003**, 2153.
- 24 B. GAERTNER, H.-J. HIMMEL, V. A. MACRAE, A. J. DOWNS, T. M. GREENE, *Chem. Eur. J.* **2004**, *10*, 3430.
- 25 H.-J. HIMMEL, L. MANCERON, publication in preparation. This molecule was previously detected in laser ablation experiments: G. P. KUSHTO, P. F. SOUTER, G. V. CHERTIHIN, L. ANDREWS, *J. Chem. Phys.* **1999**, *110*, 9020.
- 26 BP/TZVPP calculations. The structure calculated for Si<sub>2</sub>N<sub>2</sub> was compared to the one calculated previously (G. MAIER, H. P. REISENAUER, J. GLATTHAAR, *Organometallics* **2000**, *19*, 4775). Si<sub>2</sub>N<sub>2</sub> was generated and characterized in matrix-isolation experiments.
- 27 M. W. CHASE, JR., NIST-JANEF Thermochemical Tab.s, 4th Edition, *J. Phys. Chem. Ref. Data, Monograph* **1998**, *9*, 1–1951.

